Effect of grain size and material on humid granular avalanche events

Luc Oger, Claude El Tannoury, Renaud Delannay, Yves Le Gonidec, Irene Ippolito, Yanina Lucrecia Roht, Iñaki Gómez-Arriaran

Effect of grain size and material on humid granular avalanche events

Luc Oger,* Claude el Tannoury,† and Renaud Delannay‡

Univ. Rennes, CNRS, IPR [(Institut de Physique de Rennes)]-UMR 6251, F-35000 Rennes, France

Yves Le Gonidec§

Univ. Rennes, CNRS, Géosciences Rennes - UMR 6118, F-35000 Rennes, France

Irene Ippolito¶ and Yanina Lucrecia Roht**

Universidad de Buenos Aires, Facultad de Ingeniería, Grupo de Medios Porosos, Av. Paseo Colón 850, Buenos Aires Argentina

Iñaki Gómez-Arriaran††

ENEDI. Department of Thermal Engineering. University of the Basque Country - UPV/EHU, Spain

(Dated: July 12, 2018)

Abstract

Laboratory study of slope stability remains a challenge for modeling, understanding and predicting natural hasards such as avalanches and landslides. We model these phenomena by slowly and continuously tilting monodisperse dense packings of spherical beads. Three packings of glass beads of $0.2, 0.5$ and 0.75 mm diameter, and one packing of polystyrene beads of 0.14 mm diameter have been inside an ambient relative humidity ranging between 40 and 94 %. The beads fully or partially fill a transparent parallelepiped box: during tilting, displacements of the beads occur and can be captured from above and on the side of the box by two cameras. By image processing, we detect grain slides at the surface, which activity depends on humidity, bead size and material, followed by avalanches that can occur inside the box or flow outside it, depending on the pile height. These experimental results highlight that cohesive forces induced by ambient humidity have a large impact on the stability of the grain pile. The role of the exposure time to the high humidity rates is studied in order to observe the humidity diffusion process needed to reach the hygroscopic equilibrium in the packing. This behavior difference is more pronounced before the first avalanche. Indeed, the continuous tilting process avoids the observation of this effect between the next consecutive avalanches.

PACS numbers: 45.70.Ht, 61.43.Gt, 83.80.Fg

Keywords: Avalanches, precursors of avalanches, sphere packings, humidity rates

*Electronic address: luc.oger@univ-rennes1.fr

†Electronic address: claude-el-tannoury@univ-rennes1.fr

‡Electronic address: renaud.delannay@univ-rennes1.fr

§Electronic address: yves.legonidec@univ-rennes1.fr

¶Electronic address: iippoli@fi.uba.ar

**Electronic address: lucreroht@gmail.com

††Electronic address: gomez.arriaran@ehu.eus

I. INTRODUCTION

Organized granular materials displacements occur in a large range of applications like concrete, ceramic, pharmaceutical products, agricultural grains, soils and powder metallurgy. In these cases, a large amount of grains are stored, pilled or displaced by moving unstable assemblies of grains. On the other hand, grain displacements may also be observed in many natural events like debris flows, snow avalanches, ice floes and flying ashes. Understanding the physical mechanisms that control such granular structures and destabilizations is a great subject of interest for numerous industrial and environmental topics and may improve to prevent avalanches risks.

To that aim, laboratory experiments are performed with dense packings of spherical grains. Before an avalanche occurs, a large number of simultaneous displacements of grains uniformly distributed at the pile surface are the so- called precursors. Most of the experiments are performed at the laboratory scale in dry atmosphere [1–4] The aim of the present study is extending these experimental studies to wet atmospheres since moisture increases grain interaction forces and thus alters the strength of the contacts between beads. These behaviors are related to the appearance of capillary interaction which is due to the formation of liquid bridges between grains depending on the moisture content [5]. This is of first importance when dealing with natural avalanches in ambient relative humidity up to 100 %, that may exist in Argentina during several weeks. In section II, we synthesize both previous precursor-avalanche studies and previous works on the effect of humidity on grain packings.

Then, we present the reproducible technique used to prepare a good homogeneous packing (section III). In section IV, we describe the principal of the experiments used to perform extensive analysis of our experiments. Then, in section V, we measure the different local or global quantities linked to the structural evolution of the grains packings during the tilting process depending on the different experimental conditions including grain properties and box filling. In section VII we highlight the effect of the exposure time to the high humidity rates on the avalanche and precursor evolutions, the so-called "maximum stability time" or "hygroscopic equilibrium time".

II. SOME KNOWLEDGES ON THE PRECURSORS AND AVALANCHES STUDIES AND HUMIDITY EFFECTS

When tilting a granular pile, the tangential component of its weight increases inducing internal friction on its whole and leading to a superficial layer to a metastable state. When the tilt angle becomes greater than the maximum stability angle θ_A of the pile, called angle of maximum stability, the avalanche occurs. After then, the angle of the new arrangement of the granular packing decreases to the angle of repose θ_R. Pile stability is controlled by several factors, including the size of the system (height [3], length [6] width [7]), the pile density or volume compaction [1, 3, 8] and the tilting regime [9].

The destabilization of a granular pile is characterized by the rearrangements of the grains occurring at the surface of the pile. Bretz et al. [10] then Nerone et al. [4] were the first to reproduce and to film these events in a slowly inclined box. Bretz et al. [10] were interested in the presence of these events between two successive avalanches. They found that the grains reorganization distribution follows a power law in function of their size. But they didn't indicate the presence of any large event occurring between two successive avalanches. They showed that the destabilization of granular pile goes through two types of events before the avalanche: (I) small rearrangements occurring at low tilting angles, with power law size distribution function followed by (II) "Precursors" that start to appear quasi periodically when the tilt angle becomes larger than $\approx 15°$, with a non power law size distribution function . Later, several studies [6, 11, 12] were oriented to identification of the precursor of avalanches. We now go in more details in the analysis of the different criteria which control the appearanaces of both precursors and avalanches.

A. Dry avalanches

At rest, granular packings can sustain normal loads and shear stresses, such as a jammed structure, but if a threshold shear stress is exceeded, part of the material starts to flow. The discrete nature of granular materials renders their behavior very complex. Due to some external forces evolutions, the macroscopic behavior of granular media is related to the evolving geometry of their contact network and, more specifically, to the nature of the contacts themselves (frictional collisional, sliding, cohesive or not). So, for free surface flows

of granular packings under the action of gravity, the "jamming transition" above a critical shear stress is simply evidenced by the existence of the angle of maximum stability of a pile,θ_A, associated with internal friction [13]. After the flow starts, the angle of the pile relaxes towards the angle of repose, θ_R, smaller than θ_A. Similar observations were made for granular flows in a rotating drum as a function of the rotation rate [14]. Generally, experiments were performed at a low rotating regime defined as the rolling or cascading ones controlled through the Froude number "$0.05 < Fr < 0.4$ with $Fr = \omega^2 D/(2\,g)$ which represents the ratio of centrifugal to gravitational acceleration with g is the gravitational acceleration, ω the angular speed and D the diameter of a drum or the plate length [15]. As already mentioned, the behavior of inclined 3D granular media show that parameters like humidity, system dimensions, friction between grains, bottom roughness, time between avalanches or packing fraction can influence the value of the maximum angle of stability of a packing [1, 3, 6–8]. For example, Aguirre et al [1] concluded that the number of grain layers can influence the stability of a packing up to about ten layers, while it becomes independent of it for larger numbers of layers. We will see our observation of this later on in this article. Recently, few studies were developed in order to observe these phenomena. Bretz et al. [10] used a digital imaging technique to analyze the avalanches occurring during the slow inclination of a box. These large slides were separated by a sequence of rearrangements of the surface grains which were recorded by a camera. By contrast, Nerone et al. [2, 16] showed that the size of rearrangements at the surface of the packing increases with the inclination angle for freshly prepared piles filling a box. A few degrees before the avalanche starts, quasi-periodical large events are observed. Zaitsev et al [17] reported recently that the same kind of events occur in the bulk of a slowly inclined granular packing. These events were interpreted as quasi-periodic transient reorganizations of the weak-contact subnetwork occurring in the bulk of the packings. We are also studying these behaviors in our experimental setup in Rennes [18]. Staron et al. [19] investigated the evolution of the internal state of a 2D granular slope driven towards its stability limit, θ_A. They related precursors of avalanches to the intermittent mobilization of friction forces between the grains along some long-range correlations of the structure. We can summarize that precursor appearances and avalanche behaviors are mainly dependent to the grain and box sizes in one hand and to the mechanical solicitations in another hand which are both .

B. Humidity effect

In order to integrate the humidity effect in our experimental investigation, we are, firstly, collecting information through previous similar studies. For example, Gómez-Arriaran et al. [20] studied the evolution of maximum stability angles θ_A and repose angles θ_R of tilted granular pile with glass grains of size $0.5mm$, $1mm$ and $2mm$ under controlled relative humidity Φ between 5 % and 97 %. They observed that these angles are invariant in pendular state ($\Phi < 50\,\%$) which corresponds to the pore space largely filled by the gas phase and where the wetting liquid exists mainly in small isolated rings around grain contacts. Then these angles increase with relative humidity in funicular and capillary state, where the funicular state corresponds to the case where the liquid can be continuous from one area to another one in the porous space and the capillary one where the pore space is completely filled by the wetting fluid in the liquid phase.

The most important result shown in this study is that the maximum stability angle is higher in capillary state for small grain diameter, and can reach 90°. These results confirm that the cohesion between grain is better for smaller grains [21].

Some authors [22, 23] have studied the relationship between cohesion and adhesion forces between grains in a pile when an isolated ring is created between two grains contacts (I.e the external form is defined as a meniscus). These studies have established that the θ_A varies exponentially with the initial time before the experiments. Unfortunately they were performing experiments only up to $\Phi = 45\,\%$ which is far from the range over which the influence on the stability and cohesion of the granular medium is expected to be important. Other authors [24, 25] noted that the depth of the avalanche plane and the angle of repose positively correlate with the moisture content up to a maximum saturation value, which depends on the grain size only. Fraysse et al. [26] have carefully controlled Φ by injecting water vapor in a rotating drum that contained the granular medium. Thus, the control parameter to quantify the moisture content was the relative vapor pressure (P_v/P_{sat}, where P_v: vapor pressure and P_{sat}: saturated pressure), i.e., the relative humidity. They stated that θ_R slightly decreased and θ_A increased when moisture content increases.

In Mason et al. [27], a method of tilting a wet granular packing was used to determine the relationship between the angle of maximum stability θ_A and moisture, which is referred here to the volume fraction of liquid. Other authors [1, 3] also identified a relationship

between the relative humidity and the characteristic angles of an inclining box filled with $2mm$ diameter glass beads.

One of the key question of these methods is that the water is not necessarily homogeneously distributed and it was difficult to check this fact. Indeed, the rigorous control of Φ and hygroscopic equilibrium time is necessary to avoid this inhomogeneity and achieve a uniform distribution of the moisture content in the granular medium at a given hygroscopic and cohesive state. We will see this problem later on in this article.

The main difference between a dry and a wet granular medium lies in the cohesive force between grains generated by the moisture. The cohesion between two spheres [28], i.e., the attraction force between two spheres due to a liquid bridge between them, is linked to the surface tension which is the cause of the capillary pressure in the neck of the bridge. Rumpf [29] proposed a model for determining the cohesion tension in a granular medium of identical spherical grains from the force of cohesion per liquid bridge. Crassous et al. [21] have shown the evolution of the adhesive force between two grains versus distance at a given humidity rate through atomic force setup measurements.

In the continuum approach, the Mohr-Coulomb criterion describes the avalanche phenomenon in terms of shear stress (τ) and normal stress (σ) modified by the capillary condensation, which creates additional cohesion between grains, resulting in a "normal cohesive stress" in the medium (σ_c) and in a new total normal stress. This cohesive stress leads to increments in the angle of maximum stability θ_A for a wet granular packing. Indeed, as the height of the packing 'H increases, the normal stress corresponding to the weight of the pile also increases ($\rho g H$), but the cohesive forces remain constant irrespective of the size of the pile. As confirmed in Gómez-Arriaran et al. [20], if the packing depth does not influence the cohesion, failure has to occur at the base of this packing (controlled by the Mohr-Coulomb criteria) and the position will depend on the cohesion degree. In some cases, the cohesion provided by liquid bridges in the capillary cohesive state is sufficiently strong to ensure that the grains remain up to a high possible angle ($\theta_A \approx 90°$) So, when the granular medium is in funicular and pendular cohesive states, the granular medium is more appropriately considered as discrete. In this condition, all surface grains attain new stable positions which implies that the avalanche affects mainly the grains at the free surface of the packing.

According to both the continuum and discrete models, cohesive effect of liquid bridges increases the stability of the granular packing. The continuum model predicts that the

failure avalanche plan is at the bottom of the packing, and the angle of maximum stability will depend on the size of the packing. For the discrete model, the noticeable part of the failure occurs at the surface and the maximum stability angle is independent of the size of the pile. Our results in section V will confirm these two possibilities according to the different experimental conditions. Recent researches demonstrate the linear dependency between the angle of maximum stability and the time of exposition to ambient relative humidity before the avalanche [30]. Right now, we have all the elements needed to quantify the presence of the water content inside porous media on the granular packing destabilization.

III. PACKING PREPARATION AND TILTING PROCESS

To accomplish the goals of this study, an experimental setup was mounted allowing (1) the detection of the grains rearrangements at the free surface of granular pile, (2) the detection of surface angle of granular pile and (3) the control of relative humidity. The experiments consist in slowly and continuously inclining a box containing grains and following the dynamics of wet granular pile during the inclination. During this process, two independent cameras are used to record top and lateral view of the granular packing (see information below).

A. Geometrical piling

Our initial goal is the generation of dense homogeneous packings of spheres in a reproducible manner. This is crucial for having the possibility of comparing results coming from different experimental conditions. We have achieved this goal by using the so-called same "history" of the packing fabrication [31].

We are using a Plexiglas box with $6.5\,cm$ width, $11\,cm$ length and $6\,cm$ height. A grid with a mesh size twice larger then the bead diameter is initially placed at the bottom of the box. Then we fill the box with grains up to the desired height (between $2\,cm$ up to $6\,cm$). We check horizontally the packing box in order to create a quasi flat surface. Then we pull out vertically the grid to generate a homogeneous non-dense packing structure (i.e. with a packing fraction close to 0.58). When the required height is chosen as a full fill box solution, we pass a metallic bar to eliminate all the grains sitting at a position higher

than the box height. In this condition, we can assume that all our packings are made with the same history of procedure which means that they are reproducible as much as possible! When high humidity conditions are needed, all boxes were made in the same protocol then conditioned to the desired relative humidity for a given number of days in order to ensure that the liquid bridges are formed through all the granular pile (see III B). Then we place this box on top of a rotating tray. The rotation of this tray is controlled by an electrical linear actuator (Fig. 1). The inclining velocity is selected about $0.08°/s$. It is chosen after verifying that the inclination is carried out in quasi-static regime which is confirmed by the very small Froude number $Fr = 1.\,10^{-8} \ll 1.0.$. Then we began to incline the box from the horizontal position up to the maximal available angle of the setup (i.e. 75°) which can produce successive precursors or/and avalanches.

We performed our experiments by using glass grains with $0.2mm$, $0.5mm$ and $0.75mm$ diameters, and polystyrene grains with $0.14mm$ diameters.

B. Humidity control

As it was too complicate to manage a large box which can contains the packing box, the tilting setup, the horizontal camera and the vertical camera on the L-shape bar, we have decided to use the ambient conditions for low humidity rates (here up to 70%) and to manage an humidity control chamber close to the experimental setup for higher values. We can notice that we have performed our experiments in Argentina as it is sometime possible to manage experiments in natural high humidity conditions up to 100 %. During our different stays for these studies, we had only values up to 71 %. This is the reason why our tested granular piles at high humidity rates were previously conditioned during time between three weeks down to two days to desired relative humidity conditions. These conditions will allow us to observe also the evolution of the possible hygroscopic equilibrium through all the pile. This chamber is a Plexigla box which dimensions are $36\,cm$ for the width and height and $68\,cm$ for the length. This solution allows storing in the same condition up to ten packing boxes containing different experimental grain compositions (bead size or material and filling rate, among others). At the bottom of this container box is positioned a large flat plate on which is placed a saturated salt solution mixed with pure water on excess. In this manner, we can control the relative humidity in this chamber by using adequate salts

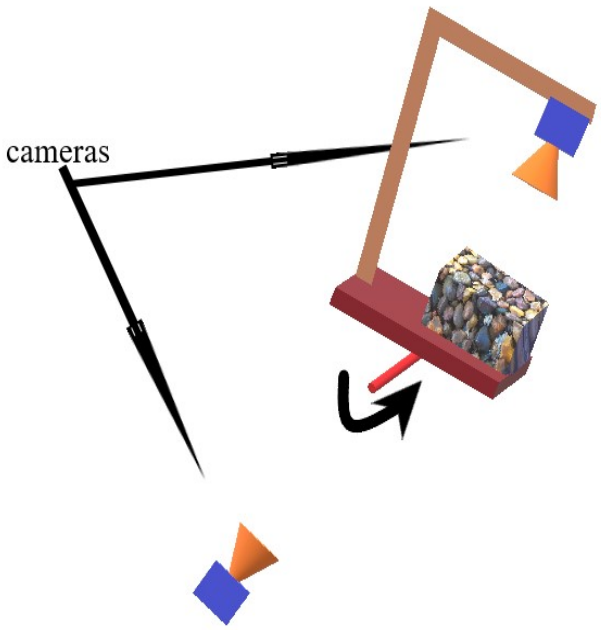

FIG. 1: Schematic view of the setup. A horizontal linear actuator is linked to a vertical bar glued to the rotating plane in order to assure the right rotation rate. A camera shooting the top surface of the packing is maintained with a L-shape bar and rotates with the rotating plane. Another camera is placed horizontally at $1\,m$ away from the moving system to record the full lateral view of the setup.

solutions with distilled water (RH for $NaCl$: $\approx 75\,\%$, KCl: $\approx 84\,\%$, KNO_3: $\approx 94\,\%$). The relative humidity and the temperature inside the chambers were recorded every 5 min by USB digital thermo-hygrometers. After the chosen "conditioning" time, we can take one box at a time and place it on the rotating tray for the experiment. The duration required for both the transfer and the full tilting experiment remains under 10 minutes, and taking in count the low velocity of the vapor diffusion process through the grain interstitials, we assume that the quality of the cohesive contacts at the free surface of the packing (mainly the top one) is not altered. This non-reversible of the humid contact breakages is one of the key difference with the Gómez et al.'s experiments [20]: the duration time of a new contact creation remains smaller than the time needed for the creation of a new capillary bridge.

IV. OPTICAL TECHNIQUES MEASUREMENTS

In order to detect the displacement of the grains, we used two cameras to film the experiment. One camera has been mounted above the free surface of the granular pile: it rotates with the tray through a L-shape bar. The other camera is not fixed on the experimental frame: it has been fixed on a tripod located one meter away from the lateral side of the Plexiglas box (Fig. 1). These two optical measurements operate quasi-simultaneously and both sets of images are processed by using the ImageJ software. In this example, the box is tilted **continuously** at a rate of $0.08°/s$

Surface angles of the granular pile are measured through the lateral video recording. Those images are registered at a frequency of 30 frames per second and a resolution of 640 by 480 pixels. The video record starts not perfectly synchronized with the surface acquisition process but it will be possible to do it after (see below). As visible in Fig. 2(a), the surface of the packing is easily detectable as having a higher grey level all along a fine visible thick line. After thresholding this grey image to generate a white band and a thinning process to create the line, a simple measurement of the mean angle of this XY pixel line can give us the surface angle. By default, due to the packing construction, this surface angle is exactly the tray angle during the initiation of the movement of the experiment (i.e. at least, up to the first event: precursor or avalanche). This allows us determining the rotation speed (slope and origin of the line) which can define the tray rotation angle during all the experiment. Figure 2(b) shows the evolution of the surface angle obtained for a packing with a $5\,cm$ height, bead diameter of $0.2\,mm$ humidity rate of $43\,\%$ for a temperature of "$26°$. When the packing reaches the first maximum stability angle, an avalanche occurs and a new surface reorganization is obtained depending of the height of the packing inside the box, the bead properties and the adhesion forces present in the experiments. In some conditions, we can observe an immediate continuous flow of grains or a new stable surface. So, in the second case, different ratchets observed here are the measurements of the successive reorganizations of the surface. This can occur more naturally before grains went outside the packing box but can also exist even when the grains exist the box (see for example Fig.4 in [20]).

Grain rearrangements at the surface that are observed at the free surface of the granular pile are recorded through the upper camera (Fig. 1) every $0.45\,s$ following the method described previously [4, 6, 12]. Image processing is based on the subtraction of two successive

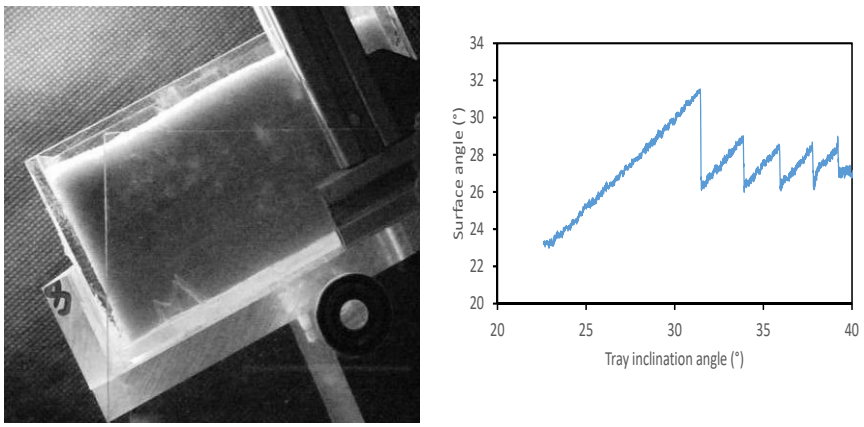

(a) (b)

FIG. 2: Lateral view and its evolution versus the tilting tray rotation for a packing with a 5 cm height, bead diameter of 0.2 mm humidity rate of 43 % for a temperature of "26°.

images thresholded higher than the image noise acquisition and produce the pixel map of moved spheres on the surface. These pixels are, by default, a direct link to at least one sphere move and allows us defining the surface S of rearranged grains. This surface can be a patchwork of isolated slots of neighboring grains or, at the end, the full surface of observation. This is the reason why we have looked a the normalization value : Indeed, this moved grains surface S is normalized by the total surface of the observation zone S_0 and plotted as a function of tilting angle (Fig. 3).

In our experiment, the largest events can represent precursors of avalanche or one of the successive avalanches. The first avalanche transition can be obtained by combining and synchronizing the two views. In Fig. 4, the two optical measurements are then plotted at the same tray inclination angle and we can easily identify avalanche events from precursor ones.

So this full optical technique analysis allows us extracting all the possible information concerning one experiment: precursor and avalanche position, interval inclination angle between precursors before the first avalanche, existence or not of precursors during the following avalanches, and so on.... The two next sections will show all the comparison results; the section V will concern only glass beads of '500 μm and the two following ones (section VI and VII) all the other conditions.

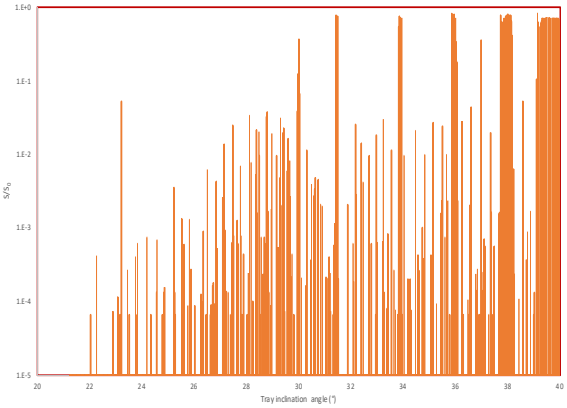

FIG. 3: Evolution of the surface fraction. The relative surface ratio is plotted in a logarithm scale in order to see the precursor amplitude evolution described by Nerone et al. [4].

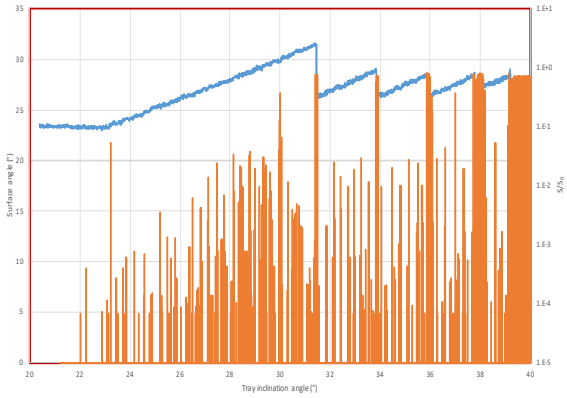

FIG. 4: Evolution of the two views with synchronization.

V. ANALYSIS OF THE RESULTS FOR $500\,\mu m$ GLASS BEADS

Several physical parameters can control our experiments such as filling height, humidity rates and conditioning times, bead sizes, bead properties, ...In the following subsections V A and V B, we will look at the effect of the filling heights and the variation of the humidity rates on the precursor and avalanche behaviors for monosize glass beads of $500\,\mu m$ diameter

only. So we will start by the filling rate.

A. Filling height effect

By opposition of the rotating drum studies, where no lower bottom wall can limit the initiation of the avalanche (i.e. only the local instability of the pile can generate the beginning of the flow), the tilting box studies, by construction, imply that a bottom wall can avoid some grain movements due to its long term geometrical influence.

1. Avalanche Analysis

According to Gómez-Arriaran et al.'s results [20], we can also observe that the successive maximum stability angles decrease after the first one and finally reach a plateau (Fig. 5). And, in the same figure, by comparison with Aguirre et al.'s observation [3], we can see the influence of the bottom wall through its number of layers order propagation. The behavior is quite different for a filling height of $2\,cm$ which corresponds to around 40 layers from higher values such as 3 or $4\,cm$ (i.e. 60 or 80 layers). This behavior is quite far from the Aguirre's experiments [1] which located the transition around 16 layers only. This difference is due to our filling process which implies a more homogeneous packing structure but with a smaller packing fraction due to the pulling out of the grid (comparison with Fig.5 in [3]). If we take into account the information from the Fig. 5 on the effective height effect on our experiments,we will focue our results for a filling rate higher than $2\,cm$.

In this case, we can observe that the maximum stability angle θ_A is increasing with the filling rate and the repose angle θ_R is also mainly decreasing with height, except for $H = 2\,cm$ where the bottom filling organization can affect the local displacement of the beads. This first behavior can be easily interpreted along the number of layers structural effect: higher number of layers means higher packing fraction due to the increase of the amount of material along the height (classically named as $\rho g H$). This fact allows less possibility of shearing ofr the lower layers.

Even if the angles θ_A is increasing and θ_R is decreasing with the filling heights, we can observe that the difference remains quite constant (Fig. 7). This observation will allow us to assume that, except for the smaller height of $2\,cm$, we can use all the results obtained

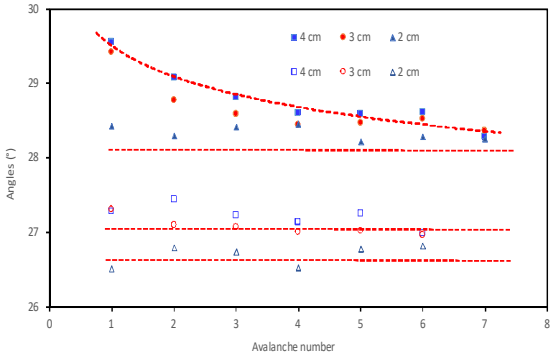

FIG. 5: Influence of the filling rates on the successive avalanche behavior. Each point is a mean average of more than ten individual runs made inside a relative humidity environment equal to $54\,\%RH$. For height equal to $2\,cm$ (≈ 40 layers) the avalanche and the repose angles are constant. For higher values (> 40 layers) we can recover the behavior visible in [20].

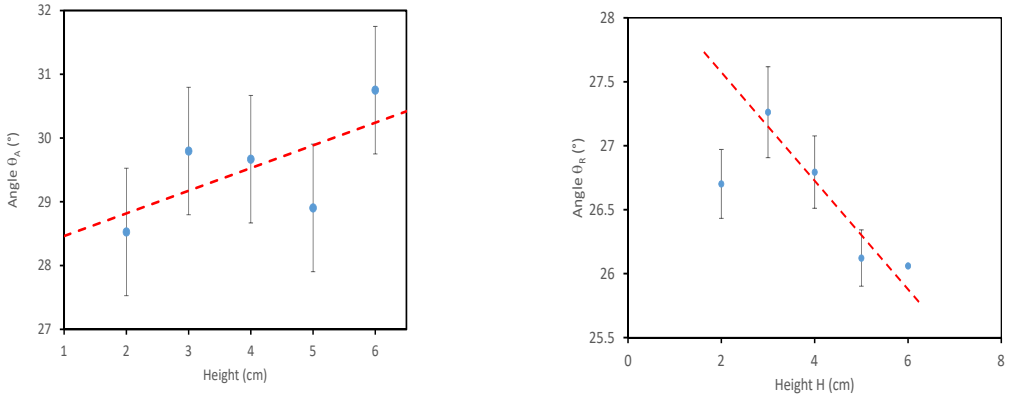

(a) (b)

FIG. 6: Evolution of the maximum stability θ_A and the repose θ_R angles for the different available filling heights. Each point is a mean average of all available data collected for all the available experiments made with an humidity rate lower than $70\,\%$ (reason is seen in Fig. 9(a)).

with different filling levels for the global analysis of the other parameter evolution.

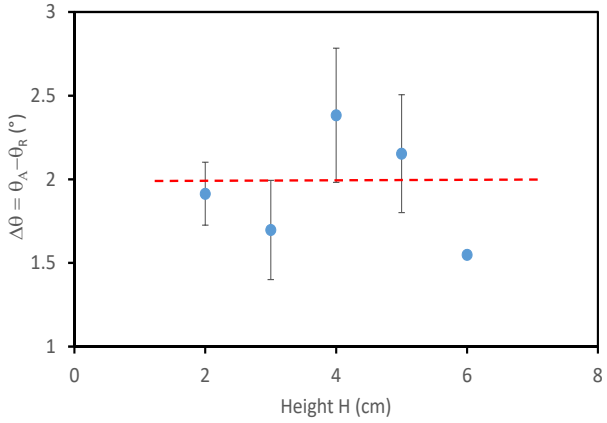

FIG. 7: Evolution of the angle difference between θ_A and θ_R versus the filling height H for experimental conditions identical at the Fig. 6.

2. Precursors Analysis

As already mentioned, the appearance of the first precursors and also the difference angle between two successive precursors is crucial to understand the structural internal interaction and to predict the following avalanche event. We can see these two informations in Fig. 8

We can see that higher the filling rate, higher the angle for the appearance of the first precursor and also the inter-precursor angle. These results can be explained in the same context of the previous observation for θ_A and θ_R: higher packing fraction for higher number of layers so less possibilities of shearing. According to these series of results, we can manage the analysis of the results for different humidities rates with the height dependency or not. Indeed this possibility can allow us to improve the different statistical behavior analysis.

B. Humidity rate (RH) effect

These experiments are performed in two different humidity conditioning behaviors depending of the range of humidities available naturally (up to 71 %) or the range of chosen ones (in our experimental cases: higher than 70 %). The change of these conditions implies automatically a change in the process before the real tilting experiments. Indeed, in the

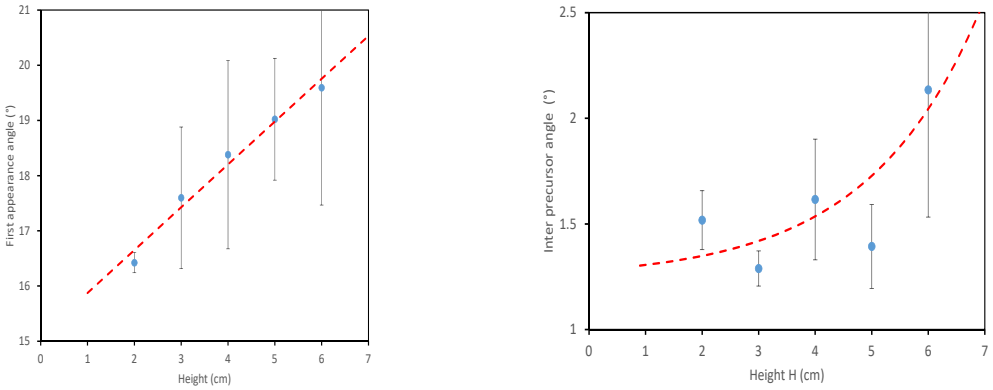

(a) (b)

FIG. 8: Evolution of the appearance angle of the first precursor versus the filling height H (a). Evolution of the inter-precursor angle versus the filling height H (b). Experimental conditions are identical at the Fig. 6.

natural case, we can assume that all the beads are naturally immersed inside the ambient humidity rate. So we don't need to maintain these build packings immobile inside a chamber before doing the experiments. By opposition, when the needed humidity rate is quite high, only samples placed inside a confined chamber saturated at the desired humidity rate during a given time can be used. In this second case, the creation of the capillary bridges inside the porous structure is, by consequence, time dependent (diffusion process inside the porous structure: see section VII).

1. Avalanche Analysis

Our first goal in this part is to reproduce as close as possible the behavior observed by Gómez-Arriaran et al. [20]. We are using the same kinds of beads ($500\,\mu m$) and also the same box dimensions (see in III) but our tilting process is quite different as it is continuous, even after the first avalanche event, at a given inclination rate by opposition of a very slow manual tilting one. The main difference is the possibility for the wet contacts to maintain a longer and stronger contact in the their set of experiments and also the ability to wait some time after a given avalanche event before performing again the tilting process. In our case,

we have try to use the smallest available titling rate in order to be close as possible to Gómez-Arriaran's experiments. Figure 9 shows that the evolution of the angles(θ_A and θ_R) follow the behavior of the Gómez-Arriaran's ones [20] except for the order of magnitude. All our results are quite smaller than their results. This fact can be easily explained by the continuous tilting which can generate higher vibrations inside the grain structure. These vibrations can more easily break some internal wet contacts and enhance the fracture propagation in our packings.

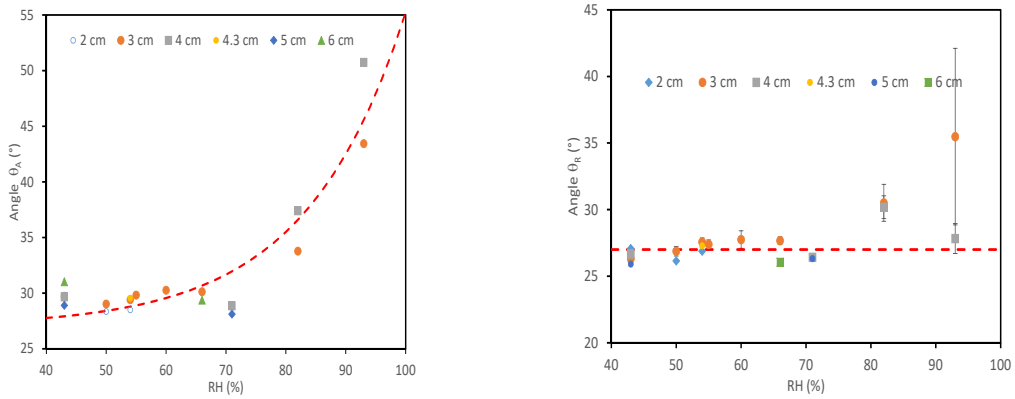

(a) (b)

FIG. 9: Evolution of the maximum stability angle θ_A and the repose angle θ_R versus the humidity rate for the different available filling heights. The results are shown separately for each set of height H. The dashed lines are only guided lines for a better observation. For (a) it is an exponential form.

More generally, we can see that the maximum stability angle θ_A is increasing significantly with the humidity rate as described in previous studies [20]. By opposition, the repose angle θ_R remains almost constant for the full range but for RH higher than 84 % an increment and a high deviation on measurements is observed, due to the underling global network of wet contacts which can play a role during the landing of the falling beads, fact which will be confirmed in the following section. The difference of behaviors between the two angles can be also seen in Fig. 10 which represents the difference between the maximum stability angle θ_A and the repose angle θ_R for all the filling height range H.

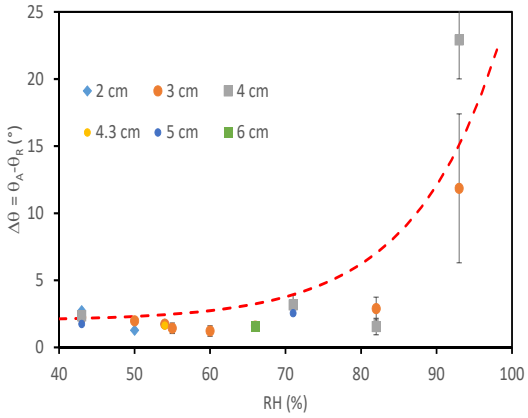

FIG. 10: Evolution of the difference between the maximum stability angle θ_A and the repose angle θ_R versus the humidity rate RH for all available filling heights H.

2. *Precursors Analysis*

As observed for the filling height effect, we can look at the influence of the humidity rate on the first appearance of the precursor and also at mean angle difference between these precursors which are present before the first avalanche (Fig. 11).

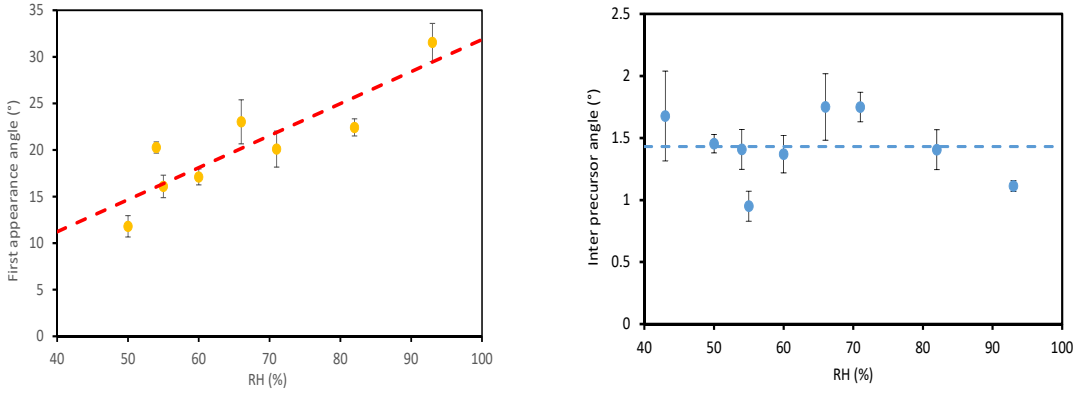

(a) (b)

FIG. 11: Evolution of the appearance angle for the first precursor versus the humidity rate RH (a). Evolution of the inter-precursor angle versus the humidity rate RH (b).

We have plotted the values for all the available filling heights used in our experiments ($H = 2$ to $6\,cm$) in order to have enough statistical observations. We can see a linear increase of the first precursor appearance with all the humidity rates even in the lower range part in which no evolution is visible for the maximum stability angle θ_A. This very interesting observation can allow us to qualify the precursor analysis as a more sensible tool for the evolution of the local adhesion force between grains. Indeed this effect is visible on the surface by the possible grain reorganization also during the precursor events. By contrast, we cannot observe a clear evolution of the inter-precursor angle value which can be explained as a phenomenon more controlled by the geometrical organization of the grain than by the adhesion force difference with the humidity rates..

VI. EFFECT OF THE BEAD SIZES AND COMPOSITION

Up to now, we have only described results obtained with beads of diameter $500\,\mu m$ which were the smallest size used by Gómez-Arriaran [20] to see the humidity influence. So to increase our range of observations; we have performed also experiments under the same mechanical and humidity conditions with glass beads of diameters $200\,\mu m$ and $750\,\mu m$ and polystyrene beads of diameter $140\,\mu m$. Firstly, we have measured for two new sets of beads the adsorption isotherms in order to observe the evolution of the water content (Fig. 12).

We can see the large increase of the water content for both beads sizes around 70 % which confirms previous results (Fig. 9). So, before this value, no big change for individual contact, or adhesion force, is possible

A. 200 μm glass beads analysis

Firstly, for the $200\,\mu m$ glass beads, we want to recover the different evolutions observed for the $500\,\mu m$ glass beads such as the angles of maximum stability θ_A and repose θ_R versus the number of avalanches then these angles versus the humidity rate and finally the first precursor appearance. For these studies, we have only performed experiments with packings which fully filled the box ($H = 6\,cm$). Indeed this filling rate was seen before in this paper as the most easy to manage.

Figure 13 shows the same behavior as the one described in Fig. 5 and in the paper of

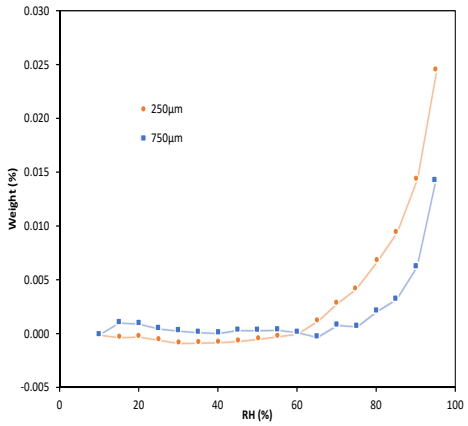

FIG. 12: Influence of the humidity rates on the adsorption isotherms for the two other beads diameters used in this study: $200\,\mu m$ and $750\,\mu m$.

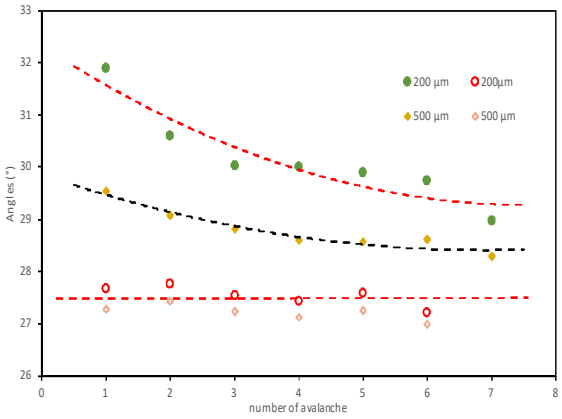

FIG. 13: Evolution of the successive avalanche behaviors for glass beads of $200\,\mu m$ (RH between 43 % and 58 %) and $500\,\mu m$ (HR between 43 % and 66 %). We can recover the classical behavior already seen before (Fig. 5) and visible in [20]. Each point is a mean value for at least 5 different runs

Gómez-Arriaran [20]. We can notify that the evolution of the angle of repose θ_R is quite similar for both diameter sizes which tends to demonstrate that the roughness of the surface

structure is not playing a crucial role. Indeed, in our case $\theta_R(200\mu m)$ is equal to $\theta_R(500\mu m)$ for all the diameter and humidity rates available.

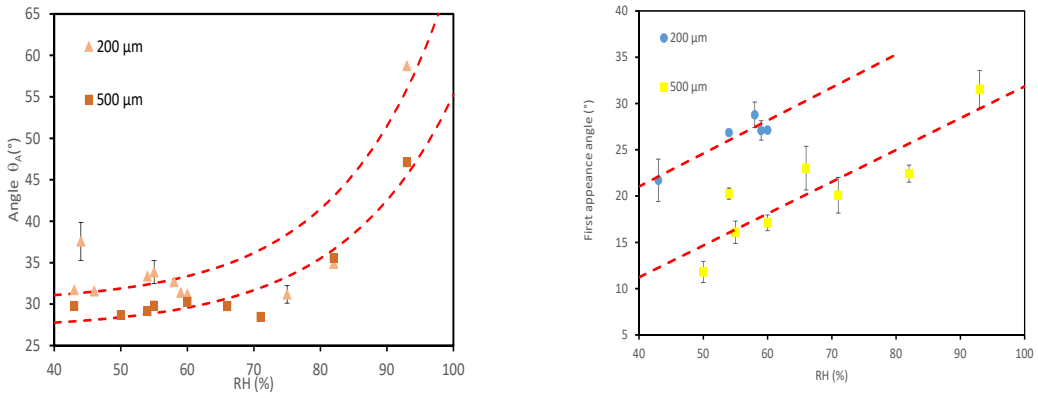

(a) (b)

FIG. 14: (a) Evolution of the maximum stability angle θ_A versus the humidity rate for a filling height $H = 6\,cm$ for glass beads of $200\,\mu m$ and $500\,\mu m$. The two dashed lines are made with the same exponential form equations. (b) Evolution of the first precursor angle versus the humidity rate for a filling height $H = 6\,cm$ for glass beads of $200\,\mu m$ and $500\,\mu m$.

Figure 14(a) shows that the behaviors of the maximum stability angles θ_A for the two bead sizes follow the same profile within this range of humidity rates. As partially seen in Fig. 13, we can also confirm that the two repose angles $theta_R$ are identical for the full range of humidity rates. In complement, the appearance angle of the first precursor is increasing with the humidity rates which confirms that this evolution is similar to the one observed for the beads of $500\,\mu m$ (fig. 11). These evolutions of the first precursor appearance in the range of humidity where the maximum stability angle seem to be quite constant are also dependent of the bead sizes which confirm us that this parameter can be a crucial indicator of real "quality" of the contacts.

B. 750 μm beads analysis

Consecutively, we have extended our studies to the $750\,\mu m$ glass beads such as the angles of maximum stability θ_A versus the humidity rate and finally the first precursor appearance

and the inter-precursor intervals. For these studies, we have also only observed experiments with packings which fully filled the box ($H = 6\,cm$). Figure 15 shows that the maximum

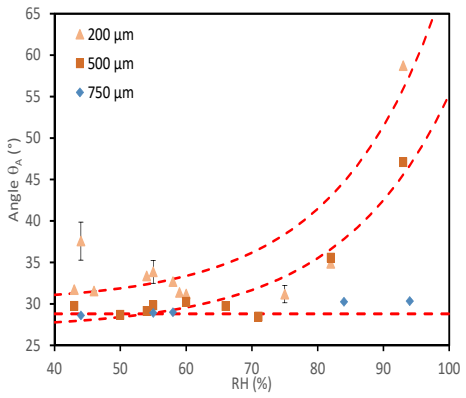

FIG. 15: (a)Evolution of the maximum stability angles θ_A versus the humidity rate for a filling height $H = 6\,cm$ for glass beads of $200\,\mu m$, $500\,\mu m$ and $750\,\mu m$. The dashed lines correspond to the two fits shown in Fig. 9 for 200 and $500\,\mu m$ and a simple horizontal linear one for $750\,\mu m$

stability angle for the $750\,\mu m$ beads is independent of the humidity rate which is quite different to the results of Gómez-Arriaran [20]. The difference of behavior is still explained by the "large" inclination speed used in our automatic setup compared to the slow manual motion used by them. Some global mechanical vibrations can strongly alter the quality of the frictional adhesive contacts especially when the water content rings around the grain contacts are weak compared to the grain weights.

Figure 16 shows that the first precursor appearance is still increasing with the humidity rate but much smaller than the results for smaller glass beads. This small increase is also a proof of the sensibility of the observation of the first precursor appearance compared to the global behavior of the maximum stability angle θ_A. In the same manner, as pointed out before, the inter-precursor interval remains constant in both cases but with different amplitudes. This amplitude difference is normal as the precursor appearances are dependent of the grain size local structure.

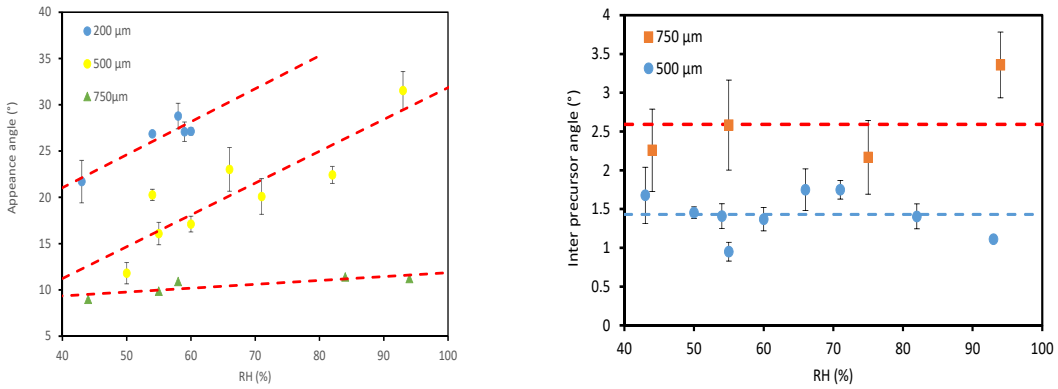

(a) (b)

FIG. 16: (a)Evolution of the first precursor angle versus the humidity rate for a filling height $H = 6\,cm$ for glass beads of $200\,\mu m$, $500\,\mu m$, and $750\,\mu m$. (b) Evolution of the inter precursor angle versus the humidity rate for a filling height $H = 6\,cm$ for glass beads of $200\,\mu m$, $500\,\mu m$, and $750\,\mu m$.

C. Polystyrene bead composition analysis

Finally, we have extended our studies to the $140\,\mu m$ polystyrene beads. These beads have a quite different water contact angle 87.4° and the critical surface tension is $40\,mN.m^{-1}$ (see in https://www.accudynetest.com) compared to 22° and $70\,mN.m^{-1}$ for glass beads respectively

We can see in Fig. 17 that the maximum stability angle of the polystyrene beads is not changing with the evolution of the humidity rate which is consistent with our expectation. Indeed, these beads are hydrophobic which means that the water meniscus at the contact point remains very small whatever the humidity rates are. So, by consequence, no increase of the adhesion forces is present and can be observed in our experiments. The linear horizontal fits for the glass beads $750\,\mu m$ and polystyrene beads of $140\,\mu m$ are identical which confirms this fact. This similarity confirms also that these maximum stability angles are almost only dependent of the disordered structure of the packing and not of the individual diameter sizes.

Figure 18 shows that the evolution of the first precursor appearance for this new set of

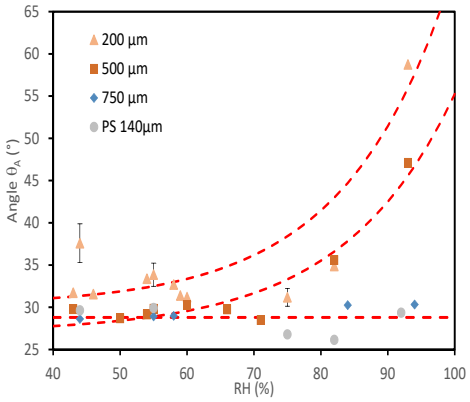

FIG. 17: Evolution of the maximum stability angles θ_A versus the humidity rate for a filling height $H = 6\,cm$ for glass beads of $200\,\mu m$, $500\,\mu m$ and $750\,\mu m$ and polystyrene beads of $140\,\mu m$. The dashed lines correspond to the fits shown in Fig. 9 for the glass beads of 200 and $500\,\mu m$ and a simple horizontal line one for $750\,\mu m$ and also for the polystyrene beads of $140\,\mu m$.

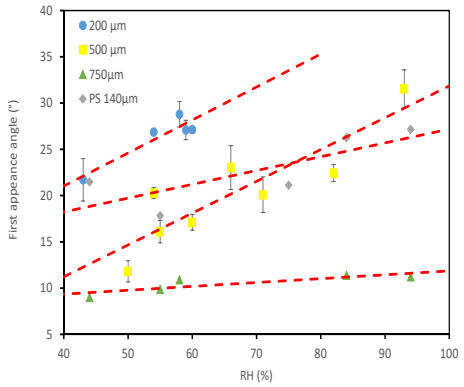

FIG. 18: (a)Evolution of the first precursor angle versus the humidity rate for a filling height $H = 6\,cm$ for glass beads of $200\,\mu m$, $500\,\mu m$, and $750\,\mu m$ and polystyrene beads of $140\,\mu m$..

beads is not following the same behavior as for the previously observed glass bead ones. This is a combination of the geometrical effect (comparison with the $200\,\mu m$ glass beads), the non wetting contact effect (comparison with the $750\,\mu m$ glass beads) and finally the different friction coefficient and mechanical properties of the two materials. These facts place the curve between the three other ones and finally confirms the quality of this "stability

indicator".

VII. EFFECT OF THE DURATION OF HUMIDITY SUBMISSION

Finally, we are dealing with a crucial parameter for our studies of the humidity effects: the quality of the humidity distribution inside the full packing. Indeed, as we are dealing with relative small beads (140 to 750 μm) the permeability of these packings are quite small which can slow down the water vapor diffusion through our static packings. As already well-known for sphere packings [32], the permeability k can be evaluated on the basis of the porosity ϕ, tortuosity factor F and mean pore size linked to the grain size D for unconsolidated beads packings ($k \propto F^{-2}\,\phi^{3/2}\,D^2$) i.e. it scales with the square of the sphere diameter.

When we have deal with natural humidity rate (i.e. up to 71% in our case), before the experiments, all the beads are lying in a dilute manner on a flat surface, so we can assume that the water is surrounding uniformly every beads according to the environmental humidity rate. So we can pack the beads inside the experimental box and start the experiment right away.

By opposition, for higher humidity rates, the packing is done previously and stored inside a given humidity rate environment. Two fans are used to ventilate the moisture inside these container boxes. This method necessitates some times to propagate the water vapor content down to the bottom of the packings. Indeed, by construction our packings have only one free accessible upper surface in contact with the moisture. As demonstrated by Gómez-Arriaran et al. [20] this waiting time is crucial for getting a perfect homogeneous adhesive structure so we are looking at our results following this particular point view. Figure 19(a) shows the evolution of the means values of the the maximum stability angles for three different samples during the avalanche processes submitted to an humidity of 94 % during either one week of or only two days.

Figure 19(b) is the representation of the angle difference of the figure(a) and the possible fit obtained from these points. So we can see a significant difference between these two behaviors which confirms that two days is largely not enough to generate an homogeneous cohesive packing. In complement, we can also mention that one week is still too small especially for small beads packings (i.e. low permeability) and high humidity rate such in this case.

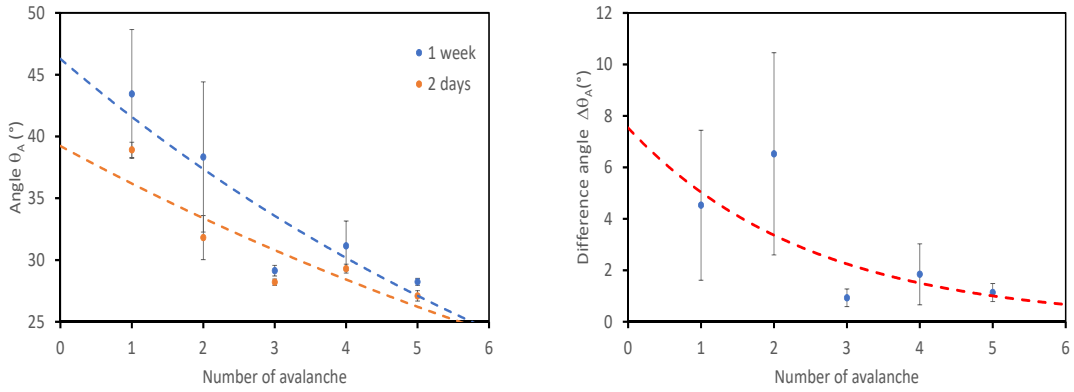

(a) (b)

FIG. 19: The maximum stability angles for two sets of packings submitted to the same humidity rate (93 %) but during two different durations (one week versus two days) (a). Difference between these two results (b)

To confirm this fact, we have also performed two sets of experiments in which the packings were immersed during four weeks or one week at an humidity rate of 82 %. In this case we have observed a relative diminution of the maximum stability angle of 17 % to be compared to the 10 % observed in the Fig. 19(b). These results are in good agreement with the two papers of Gómez-Arriaran et al. [20, 30] showing that a minimal duration of two weeks is needed in order to propagate through all the samples the moisture in order to generate uniform adhesion forces for all the contacts available inside the packings.

VIII. CONCLUSION

So in conclusion, we have presented here a study to characterize the influence of the humidity rates on the rearrangement events (precursors and avalanches) inside sphere packings when they are inclined slowly and continuously up to the final granular avalanche.

Studies reported before have shown the evolution of the successive avalanches which occurred during these tilting processes. In complement, other studies have demonstrated the existence of precursor events such surface rearrangements of grains before an avalanche: small (few individual grains in movement) and large rearrangements or precursors (number

of displaced grains of the order of one or more packing layers). We have confirmed all these previous results, but here we have also demonstrated that these precursors (first appearance and periodicities) are depending to the grain size, grain properties and, more important, of the inner humidity rates. Indeed, the precursor observations have a more precise fluctuation according to the humidity rates changes than the other classical avalanche parameters.

IX. ACKNOWLEDGMENTS

This work was partially done during the LIA CNRS PMF and the ECOS-SUD E15A043 programs. A grant for external exchange of PhD student was also obtained by C. el Tannoury in order to perform experiments during two months in GMP-UBA. I. Gómez-Arriaran thanks the Laboratory of Quality Control in Buildings, of the Department of Environment, Territorial Planning and Housing of the Basque Government.

---

[1] M.A. Aguirre, N. Nerone, A. Calvo, I. Ippolito, and D. Bideau. Influence of the number of layers in the equilibrium of a granular surface. *Physical Review E*, 62(1):738–743, 2000.

[2] N. Nerone, M.A. Aguirre, A. Calvo, I. Ippolito, and D. Bideau. Surface fluctuation in a slowly driven granular system. *Physica A*, 283:218–222, 2000.

[3] M.A. Aguirre, N. Nerone, A. Calvo, I. Ippolito, and D. Bideau. Granular packing: influence of different parameters on its stability. *Granular Matter*, 3:75–77, 2001.

[4] N. Nerone, M.A. Aguirre, A. Calvo, D. Bideau, and I. Ippolito. Instabilities in slowly driven granular packing. *Phys. Rev. E*, 67:011302, 2003.

[5] E. Charlaix and M. Ciccotti. chap. 12 capillary condensation in confined media. In K. D. Sattler, editor, *Handbook of Nanophysics: Principles and Methods*. CRC Press, Boca Raton, FL, 2010.

[6] S. Kiesgen de Richter, G Le Caër, and R. Delannay. Dynamics of rearrangements during inclination of granular packings: the avalanche precursor regime. *J. Stat. Mech.*, page 04013, 2012.

[7] P. Boltenhagen. Boundary effects on the maximal angle of stability of a granular packing. *The European Physical Journal B*, 12(1):75–78, oct 1999.

[8] P. Evesque, D. Fargeix, P. Habib, M. P. Luong, and P. Porion. Gravity and density dependences of sand avalanches. *J. Phys. I France*, 2:1271, 1992.

[9] A. Jarray, V. Magnanimo, and S. Luding. Wet granular flow control through liquid induced cohesion. *Powder Technology*, feb 2018.

[10] M. Bretz, J. B. Cunningham, P. L. Kurczynski, and F. Nori. Imaging of avalanches in granular materials. *Physical Review Letters*, 69(16):2431–2434, oct 1992.

[11] M. Duranteau, V. Tournat, V. Zaitsev, R. Delannay, and P. Richard. Identification of avalanche precursors by acoustic probing in the bulk of tilted granular layers. In *Powders and Grains 2013: Proceedings of the 7th International Conference on Micromechanics of Granular Media*, volume 1542, page 650. AIP, 2013.

[12] M. Duranteau, R. Delannay, P. Richard, and V. Tournat. Avalanches and quasi-periodic events in slowly tilted granular media. *Journal of Statistical Mechanics*, 2014.

[13] Y. Zhang and C. S. Campbell. The interface between fluid-like and solid-like behaviour in two-dimensional granular flows. *J. Fluid Mech.*, 237:541, 1992.

[14] R. Fischer, P. Gondret, and M. Rabaud. Transition by intermittency in granular matter: From discontinuous avalanches to continuous flow. *Physical Review Letters*, 103(12):128002, sep 2009.

[15] J. Litster and B. Ennis. *The Science and Engineering of Granulation Processes*. Springer Netherlands, 2004.

[16] N. Nerone and S. Gabbanelli. Surface fluctuations and the inertia effect in sandpiles. *Granular Matter*, 3(1-2):117, jan 2001.

[17] V. Yu. Zaitsev, P. Richard, R. Delannay, V. Tournat, and V. E. Gusev. Pre-avalanche structural rearrangements in the bulk of granular medium: Experimental evidence. *EPL (Europhysics Letters)*, 83(6):64003, sep 2008.

[18] Y. Zhu, C. el Tannoury, R. Delannay, L. Oger, and Y. Le Gonidec. Precursors periodicity during cycling of oscillated sphere packings. *J. Phys. D: Appl. Phys.*, page preprint, 2018.

[19] L. Staron, F. Radjai, and J.P. Vilotte. Granular micro-structure and avalanche precursors. *Journal of Statistical Mechanics: Theory and Experiment*, 2006(07):P07014–P07014, jul 2006.

[20] I. Gómez-Arriaran, I. Ippolito, R. Chertcoff, M. Odriozola-Maritorena, and R. De Schant. Characterization of wet granular avalanches in controlled relative humidity conditions. *Powder Technology*, 279:24–32, jul 2015.

[21] J. Crassous, M. Ciccotti, and E. Charlaix. Capillary force between wetted nanometric contacts and its application to atomic force microscopy. *Langmuir*, 27:3468–3473, 2011.

[22] F. Restagno, L. Bocquet, and E. Charlaix. Where does a cohesive granular heap break? *The European Physical Journal E*, 14(2):177–183, jun 2004.

[23] L. Bocquet, E. Charlaix, S. Ciliberto, and J. Crassous. Moisture-induced ageing in granular media and the kinetics of capillary condensation. *Nature*, 396(6713):735–737, dec 1998.

[24] A. Samadani and A. Kudrolli. Angle of repose and segregation in cohesive granular matter. *Physical Review E*, 64(5):051301, oct 2001.

[25] S. Nowak, A. Samadani, and A. Kudrolli. Maximum angle of stability of a wet granular pile. *Nature Physics*, 1(1):50–52, oct 2005.

[26] N. Fraysse, H. Thomé, and L. Petit. Humidity effect on the stability of a sandpile. *The European Physical Journal B*, 11(4):615–619, oct 1999.

[27] T. G. Mason, A. J. Levine, D. Ertaş, and T. C. Halsey. Critical angle of wet sandpiles. *Physical Review E*, 60(5):5, nov 1999.

[28] C. D.Willett, M. J. Adams, S. A. Johnson, and J.P.K. Seville. Capillary bridges between two spherical bodies. *Langmuir*, 16(24):9396–9405, nov 2000.

[29] H. Rumpf. *The strength of granules and agglomerates*, pages 379–418. Interscience Publishers, New York, 1962.

[30] I. Gómez-Arriaran, I. Ippolito, R. Chertcoff, M. Odriozola-Maritorena, and Y.L. Roht. Dynamic behavior of wet granular media under variable humidity conditions: characteristic stability time. *submitted*, 2018.

[31] D. Bideau, E. Guyon, and L. Oger. Granular media: Effects of disorder. In J. C. Charmet, S. Roux, and E. Guyon, editors, *Disorder and Fracture*. Springer US, 1990.

[32] E. Guyon, L. Oger, and T.J. PLona. Transport properties in sintered porous media composed of two particle sizes. *Journal of Physics D: Applied Physics*, 20(12):1637–1644, dec 1987.